J. Min. Metall. Sect. B-Metall. 58 (2) (2022) 191 - 202

Journal of Mining and Metallurgy, Section B: Metallurgy

CHARACTERIZATIONS AND GROWTH KINETICS OF THE BORIDED LAYER FORMED ON PURE NICKEL BY MOLTEN SALT ELECTROLYSIS

B.-X. Wang*, W.-L. Yuan, Z.-Y. Wang, J.-X. Li, H.-Z. Ma, Y.-H. Song

Xi'an University of Architecture and Technology, School of Metallurgical Engineering, Xi'an, China

(Received 01 November 2021; Accepted 09 April 2022)

Abstract

Molten salt electrolysis was applied for the boronizing of nickel with $Na_2B_4O_7{\cdot}10H_2O$-Na_2CO_3 as the electrolyte and characterizations and the growth kinetics of borided layer is reported. The experiment was carried out in silicon carbide crucible at 1193 K, 1223 K, and 1243 K for 1 h, 2 h, 3 h, and 4 h. The morphology and phases formed on the surface of pure nickel were analyzed by means of scanning electron microscopy (SEM), energy dispersive X-ray spectroscopy (EDS), and X-ray diffraction analysis (XRD). The surface hardness and corrosion resistance of the boronized sample were tested by micro hardness tester and electrochemical workstation, respectively. The borided layer was composed of nickel borides and its thickness ranged from 71 to 184 μm. After 1 h of boronizing, the hardness of the silicon rich borides is 966 HK, which is a little lower than that of the nickel borides (992-1008 HK); the surface hardness reached 1755 HK after 4 h electrolysis. Electrochemical impedance spectroscopy analysis showed that the corrosion resistance of boronized sample is better than that of pure nickel. Borided layer growth kinetics was studied by analyzing the relationship between thickness of the borided layer and time by mathematical method. Then the diffusion coefficient constant of boron atom in nickel at 1193 K, 1223 K and 1243 K was calculated accordingly and an equation was obtained to estimate the thickness of the borided layer.

Keywords: *Pure nickel; Boriding; Molten salt electrolysis; Kinetics; Surface hardness*

1. Introduction

Nickel and Nickel-base alloys have been widely used in aviation, military, civil machinery manufacturing, battery materials, and nickel plating industry for their high strength, good plasticity and machining property, and high-temperature corrosion resistance. However, the low surface hardness and low wear resistance of nickel limit the further expansion of its application fields [1]. For this reason, it is necessary to enhance their surface hardness and wear resistance through surface hardening treatments.

Boriding is a thermo-chemical surface treatment process in which boron atoms diffuse into a metal substrate and form one or more hard boride layers on the metal surface [2]. As the metal borides layers formed have higher hardness and wear resistance than the metal matrix [3, 4], the boriding has been a metal surface heat treatment process developed and applied in industry in recent years [5].

The traditional boronizing processes include gas boronizing [6-8], paste boronizing [9], plasma paste boriding [10-12], powder pack boronizing [13-16], and electrochemical boronizing [2] etc.Electrochemical boriding was originally developed by Ornig and Schaaber in 1940s [15]. Despite being a very old process, attempts to study the thermodynamics and kinetics of electrochemical boriding process did not start until 1980s. From then on, boronizing of various alloys and metals such as low carbon steel [18, 19], iron [20], titanium [2] and also nickel-based alloys [21] by molten salt electrochemical boriding have been studied. This method has a series of advantages such as simple agents, low cost, convenient operation, low pollution, and repeatable application of the agent [22-23]. V. Sista [21] used anhydrous borax and sodium carbonate as boronizing agents to boronize Inconel 600 by molten salt electrolysis, and obtained a layer with the thickness of 30-80 μm, including NiB, Ni_2B, Ni_3B, Ni_4B_3 and other nickel-boron compounds, and its hardness is much higher than that of nickel-based alloy.

At present, there are few studies on the reaction mechanism and kinetics of nickel boronizing process by molten salt electrolysis. In this study, the pure nickel was borided considering the advantages of molten salt electrolysis boronizing process. The aim of this study is to analyze the formation principle of the nickel borides, and to investigate the growth kinetics of the borided layer on pure nickel. The morphology of the borided layers was examined by

*Corresponding author: yj-wangbixia@xauat.edu.cn

https://doi.org/10.2298/JMMB211101003W

SEM, the distribution of elements in their zones was investigated by the EDS analysis, and the nature of electrochemical reactions was studied by using the cyclic voltammetry. In addition, based on the growth kinetics study of the boride layers in the temperature range of 1193-1243 K, an equation was obtained to estimate the thickness of the borided layer at 1223 K.

2. Experimental

Commercially available nickel N6 (NNS N02200) plates (nominal composition of Cu 0.06 wt.%, Mn 0.05 wt.%, S 0.005 wt.%, Fe, C, Si are all 0.10 wt.%, and balance Ni+Co) were obtained from a commercial source, and they were cut into 10 mm × 40 mm × 3 mm rectangular pieces to fit into the electrochemical boriding unit.

The nickel pieces were ground and polished to 1200 grit size SiC emery papers to remove the surface oxide layers and other contaminants from the surface. The samples were then cleaned with alkali for 1/4 h and soaked in acid for 1/12 h to remove oil and rust respectively. The alkali solution was prepared by NaOH 15 g/L, Na_2CO_3 25 g/L, H_3PO_4 60 g/L, $NaSiO_3 \cdot 9H_2O$ 10 g/L and heated to 333 K. The rust removal solution was prepared with 4 % HF and 20 % HNO_3 and used at room temperature.

The electrochemical boriding experiments were carried out in molten borax based (85% $Na_2B_4O_7$+15% Na_2CO_3) electrolyte in a silicon carbide (SiC) crucible at 1193 K, 1223 K and 1243 K, for different durations, with a current density of 750 mA/cm^2. The nickel pieces acted as the cathode while a graphite rod served as the anode. While in the electrochemical study, a tungsten wire was used as the working electrode, a platinum wire was used as the reference electrode and a graphite rod acted as the counter electrode. The cyclic voltammetry was employed to understand the electrochemical reactions involved during electrolysis in a molten borax based (85% $Na_2B_4O_7$+15% Na_2CO_3) electrolyte, using a PARSTAT 4000 multichannel electrochemical workstation.

85% $Na_2B_4O_7 \cdot 10H_2O$ and 15% Na_2CO_3 were uniformly mixed and dried, ground to 75 μm, and put into SiC crucible. The crucible was put into a sealed reactor, and then the reactor was heated in the resistance furnace. When the molten salt was completely melted, the nickel sample was immersed into the electrolyte. The experiment was carried out in an argon atmosphere. After electrolysis, the boronized sample was taken out and air cooled to room temperature.

The boronizing experimental device was shown in Figure 1.

Gemini SEM 300 field emission scanning electron microscopy (SEM) was used to observe the cross-sectional morphology of the boronized samples, and the distribution of elements in the boronized layer was analyzed by a supporting energy dispersive spectroscopy (EDS). The phase composition analysis

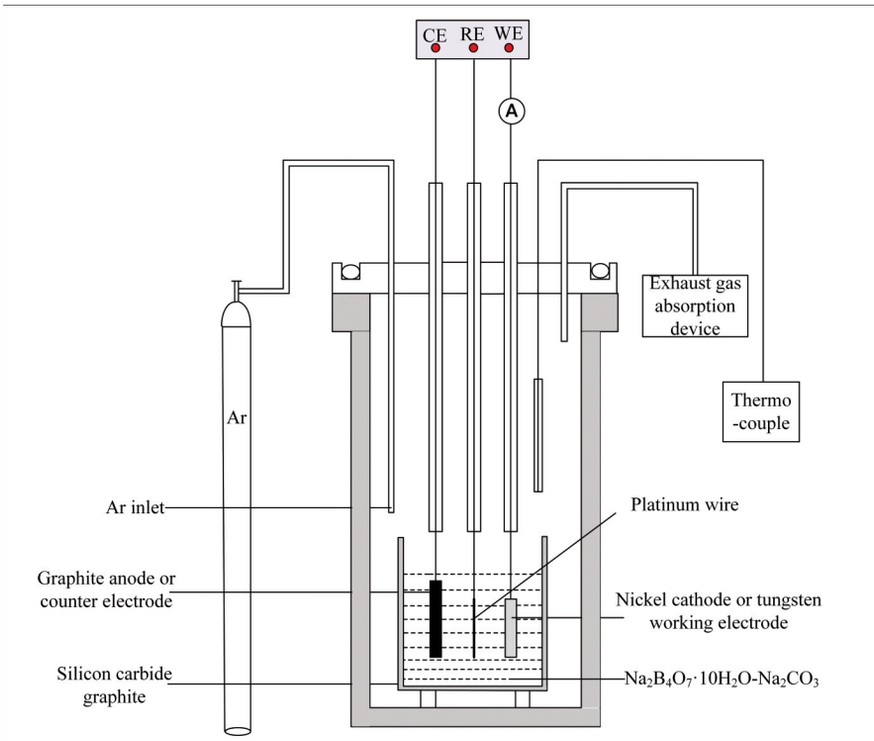

***Figure 1**. Schematic diagram of the experimental device*

of the borided sample was performed by Empyream Sharp X-ray Diffraction (XRD). The anode target was Cu target, and the scanning angle was 20~90°. The wavelength of Kα ray is 0.15406. The thickness of boronizing layer was determined according to the mechanical industry standards JB/T4215-2008 (Boronizing) and JB/T7709-2007 (Detection methods for microstructure, hardness, and layer depth of boronized layer). The surface hardness of Nickel matrix and the boronized samples were measured by MHV-1000 digital display microhardness tester. The load pressure was 0.245N and the hold time was 20s.

The corrosion resistance of pure nickel and the boronized samples in 3.5% NaCl solution was investigated by electrochemical impedance spectroscopy (EIS) and polarization curve (Tafel) using PARSTAT 4000 electrochemical workstation.

3. Result and discussion

3.1. X-ray diffraction studies

XRD study on the surface of the borided nickel samples was carried out, the resulting XRD patterns were shown in Figure 2. Based on the XRD data, we concluded that the surface of the borided layer is mainly composed of nickel borides such as Ni_2B and Ni_3B phases. These phases have tetragonal and orthorhombic crystal structures, respectively. As the temperature increased from 1193 K to 1243 K, the diffraction peaks of Ni_2B and Ni_3B phases became stronger and sharper in the X-ray diffraction spectra, which indicates that the crystal of the nickel borides grow quickly at a higher temperature due to a higher diffusion rate of boron atoms. In addition, the peaks of NiB and Ni_4B_3 also appeared in the XRD patterns, and the peaks became stronger at a higher temperature of 1243K. The presence of NiB and Ni_4B_3 in the boriding of nickel was also reported by V. Sista [21] and I. Gunes [1] using electrochemical boriding and powder packing boriding, respectively.

3.2. Morphology of the borided layers

The cross-sectional morphology of the borided layers formed on nickel were examined by SEM. Figure 3 shows the SEM images of the borided layers formed at 1223 K for process duration of 1, 2, 3, and 4 h, respectively.

It can be seen from the Figure 3 that the structure of the borided layers looks very dense. Unlike borided layers produced by conventional powder pack methods, it does not have a dendritic or tooth-like structure [22]. The thickness of the borided layers increases with the extension of electrolysis time.

Note that there are two zones in the borided layer: a thinner outer zone and a thicker inner zone, hence EDS was carried out on sample in Figure 3 (a) to reveal the elements and their distribution in the borided layer and the results was shown in Figure 4.

It was found in Figure 4 that Ni, B, Si and C were detected in the borided layer. Si concentrated in the outer zone while the content of B decreased along the vertical line from the outer layer to the inner layer and then to the substrate. This is because the diffusion distance of boron atom increases with the increase of the thickness of the borided layer. The source of silicon was speculated to be the silicon carbide crucible used in the experiment. Nickel and boron were evenly distributed in the inner zone with the average weight percentage of boron element in zone 2 being 11.56%. According to the phase diagram for nickel-boron alloy [25] , when the weight percentage of boron is about 6% and 8%, Ni_3B and Ni_2B can be formed respectively. When the weight percentage of boron increases from 12% to 15%, the phases of o-Ni_4B_3, m-Ni_4B_3 and NiB will be formed in sequence. As Ni_3B,

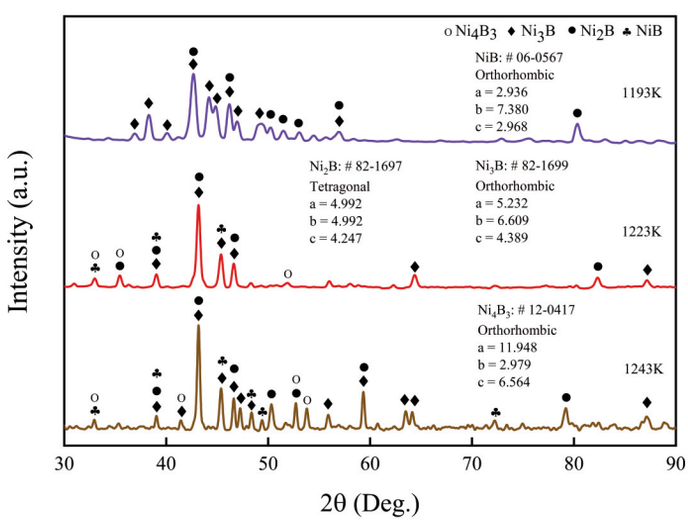

Figure 2. *XRD patterns in the surface of the boronized sample (1193 K, 1223 K and 1243 K, 750 A/m², 1 h)*

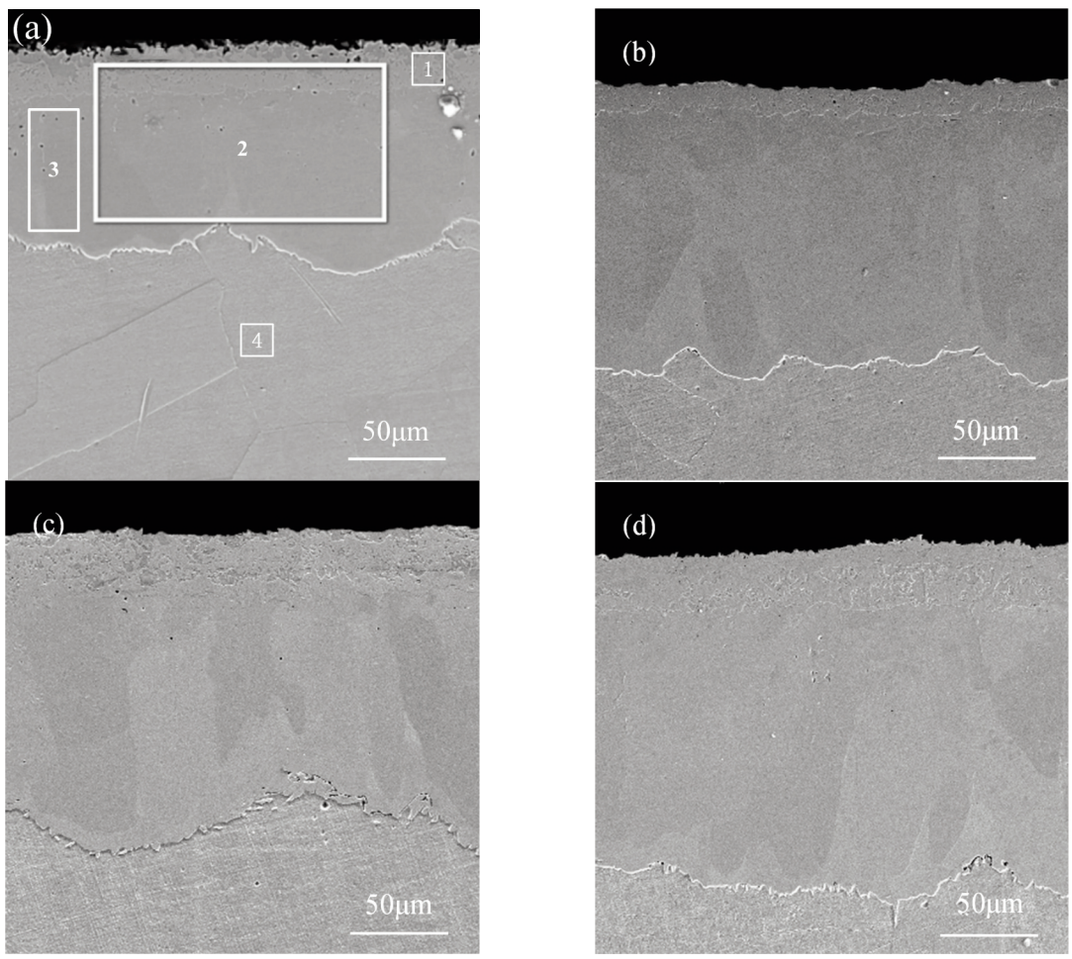

Figure 3. *Cross-sectional SEM images of the boronized sample at different electrolysis time (1223 K, 750 A/m²) (a) 1 h (b) 2 h (c) 3 h (d) 4 h*

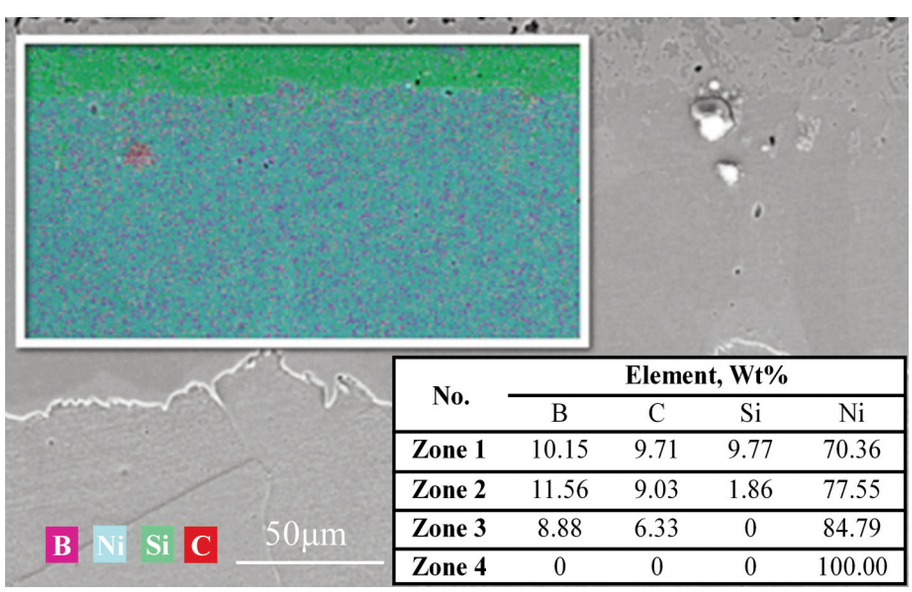

No.	Element, Wt%			
	B	C	Si	Ni
Zone 1	10.15	9.71	9.77	70.36
Zone 2	11.56	9.03	1.86	77.55
Zone 3	8.88	6.33	0	84.79
Zone 4	0	0	0	100.00

Figure 4. *The elements distribution in the borided layer(zone 2 in Figure3a) and element centent in different zones in Figure 3a (1223K, 750A/m², 1 h)*

Ni_2B, NiB, and Ni_4B_3 coexisted in zone 2, the average boron content in this zone was 11.56%.

In Ref [24], SiC (weight percentage 88%) was used in the powder mixture (B_4C, KBF_4 and SiC) as a diluent during borosiliconizing of 99.9% pure nickel. As a consequence, the multicomponent layers containing nickel silicides (Ni_2Si, Ni_3Si or Ni_5Si_2) and nickel borides were produced. The thickness of the nickel silicides reached 230 μm when borided at 1223 K for 8 h. As the amount of SiC in this experiment is much lower than that used in Ref [24], no silicides were formed in the upper layer and the nickel borides in this layer were rich in silicon. The thickness of the nickel borides rich in silicon was about 43 μm while the total thickness of the borided layer was 184 μm after electrolytic boriding at 1223K for 4 h.

As to the presence of carbon in the borided layer, it may be attributed to the graphite anode and Na_2CO_3 containing molten salt used in the experiment. The source of carbon and the methods to remove it from the borided layer need further research.

3.3. Thickness and hardness analysis

Figure 5 is the plots of the thickness and surface hardness of the borided sample with respect to the boriding time. These samples were borided at 1223 K for 1, 2, 3, and 4 h, respectively.

It can be seen in Figure 5 (a) that with the increase of electrolysis time, the thickness of the borided layer increases. When the electrolysis time is 1 h, the thickness of the borided layer is about 71 μm. The thickness of the borided layer reaches 184 μm after 4 h. However, the growth rate of the borided layer decreases with electrolysis duration. At the initial stage of boronizing, the continuous thermal decomposition reaction, electrochemical reaction, and reduction reaction in molten salt system at high temperature make the generated active boron atoms continuously diffuse into the surface of nickel matrix and form borides with nickel, so that the thickness of the borided layer increases at a faster rate. With the extension of electrolysis time, the nickel surface was covered by a layer of nickel borides, so the newly generated boron atoms must diffuse through the covered layer to reach the nickel substrate. The thicker the covered layer is, the longer the diffusion distance is, resulting in the slower growth rate of the borided layer in the later stage of electrolysis boriding.

In Figure 5 (b), the surface hardness of the borided sample also increases with boriding duration. After 4 h of electrolysis, the surface hardness of the sample is about 1755 HK, and this value is about 8.7 times that of the nickel matrix (199 HK).

Figure 6 shows the hardness in the cross-section of the sample borided for 1 h. It can be observed that the hardness of the silicon rich borides layer (966 HK) in

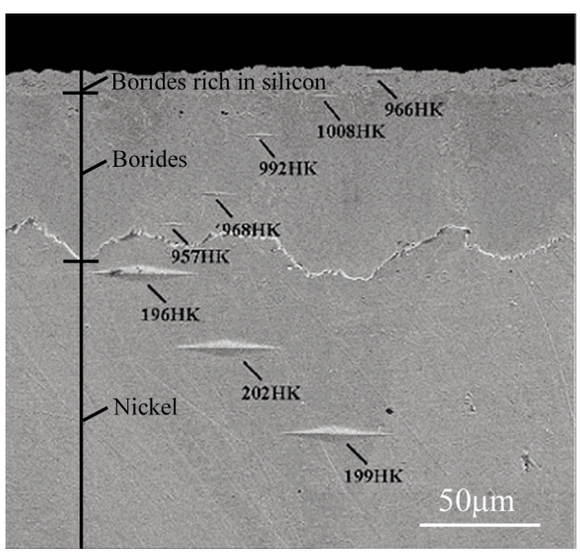

Figure 6. *Hardness in the cross-section of the borided sample (1223K, 750A/m² ,1 h)*

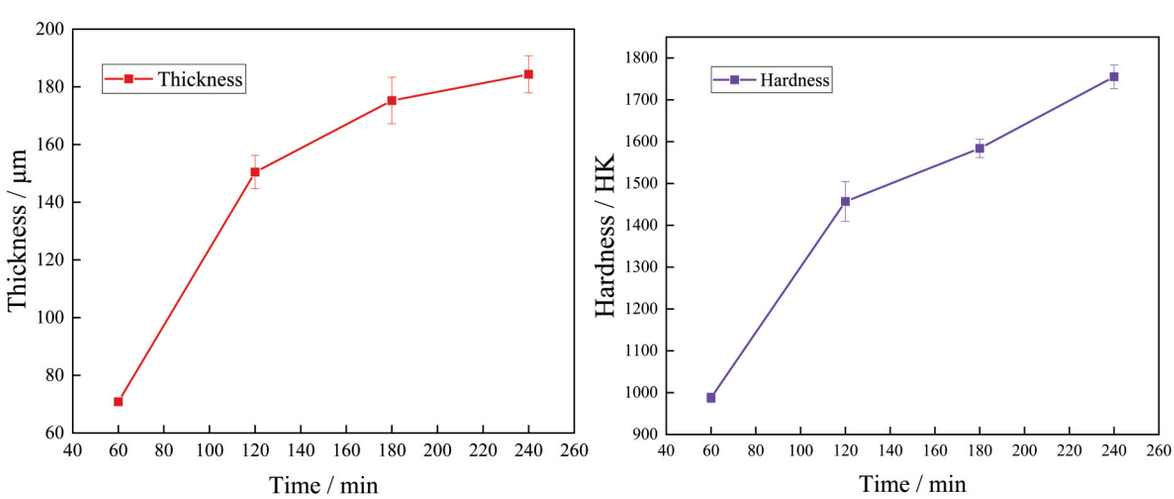

Figure 5. *Variations of thickness of the borides layer (a) and surface hardness of the boronized sample (b) with time*

the upper zone is a little lower than that of the nickel borides (992-1008 HK) in the inner zone. The hardness near the interface between nickel borides and nickel substrate decreases to 957 HK, while the hardness of the nickel substrate is around 199 HK. The change of hardness in the borided layer is in accordance with that in Ref [24], where in the zone of nickel silicides, the thickness is about 230 μm and the hardness is HV 832, while the zone of nickel borides was characterized by a higher hardness of HV 984 and a thinner thickness of about 20 μm. Hence, silicon should be avoided in the boride layer with regard to improving the hardness of the borided layer.

3.4. Corrosion resistance

The electrochemical impedance spectroscopy test and potentiodynamic polarization test were conducted on pure nickel and the borided sample, which was boronized for 3 h at 1223 K, with a boride layer of about 175μm in 3.5% NaCl solution at room temperature to investigate the electrochemical corrosion behavior. Figure 7 shows the electrochemical impedance spectroscopy test results.

It can be observed from Figure 7 that for the borided sample, its Nyquist diagram has capacitive arc characteristics and the radius of capacitance in the electrochemical impedance spectroscopy is larger than that of pure nickel, which indicates that the boronized sample can form a dense and stable passive film in solution, the corrosion resistance of the boronized sample is better than that of pure nickel.

Figure 8 shows the dynamic potential polarization curve of pure nickel and the boronized sample in 3.5 % NaCl solution. For pure nickel, the anodic polarization started when the corrosive potential was -0.46 V, then with the increase of potential, the anodic dissolution went on until the corrosive potential reached -0.06 V. Beyond this point, the nickel anode was kept passivated in the solution, while for the borided sample the anodic dissolution started at the potential of -0.32 V and the anodic passivation started at 0.52 V.

The electrochemical parameters of the samples can be obtained from Figure 8 by curve fitting method and were shown in Table 1. In Table 1, βa and βc (V) represent the Tafel slope of anode and cathode respectively. i_{corr} (A/cm^2) is self-corrosion current density, which can be deduced from Figure 8. Rp (R) represents polarization resistance and can be calculated by Stern-Geary formula (Eq (1)). E_{corr} (V) are self-corrosion potential. Corrosion rate of the sample can be calculated by Eq. (2) [26].

$$R_p = \frac{\beta_a \beta_c}{2.303 i_{corr}(\beta_a + \beta_c)} \quad (1)$$

$$Corrosion\ rate = \frac{M \cdot i_{corr}}{n \cdot F \cdot \rho} \quad (2)$$

Where, M is the atomic weight or molecular weight of the sample, n is the number of electron transferred in electrochemical reaction, F is Faraday constant, and is the density of the sample.

Based on the electrochemical corrosion principle that for a sample, the more positive the self-corrosion potential is and the smaller the self-corrosion current density is, the slower the corrosion rate will be; the greater the polarization resistance and the more stable the passivation film is, the better the corrosion performance of the sample will be. Therefore, it can be concluded from Table 1 that the corrosion resistance of boronized samples is much higher than that of pure nickel, which is attributed to the nickel borides formed on the surface of nickel.

3.5. Boronizing mechanism

In the former work, the formation of boron in

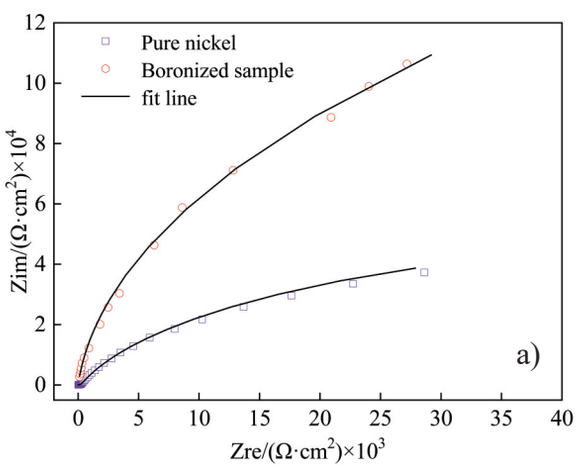

Figure 7. *Nyquist spectrum for pure nickel and boronized sample*

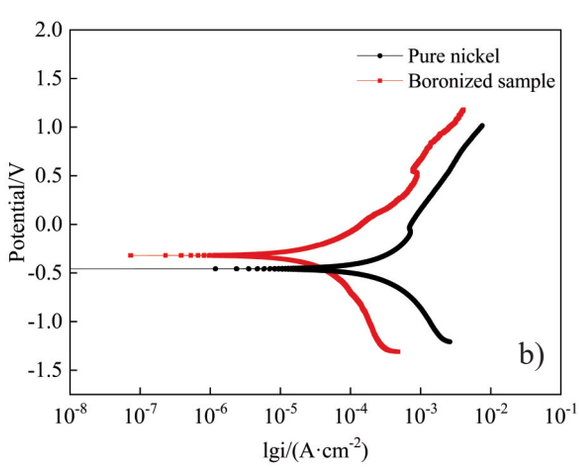

Figure 8. *Polarization curve of pure nickel and the boronized sample in 3.5% NaCl solution*

$Na_2B_4O_7$ system and $Na_2B_4O_7$ - Na_2CO_3 system was studied by thermal analysis and cyclic voltammetry [22-23]. The formation reactions of boron in $Na_2B_4O_7$ molten salt were Eqs (3) - (10), while those in $Na_2B_4O_7$ - Na_2CO_3 system were shown in Eqs (6) - (8) and Eqs (9) - (10).

$$Na_2B_4O_7 + Na_2CO_3 = 4NaBO_2 + CO_2 \quad (3)$$

$$NaBO_2 = Na^+ + BO_2^- \quad (4)$$

$$2BO_2^- = B_2O_3 + 1/2O_2 + 2e^- \quad (5)$$

$$Na_2B_4O_7 = Na_2B_2O_4 + B_2O_3 \quad (6)$$

$$Na_2B_2O_4 = 2Na^+ + B_2O_4^{2-} \quad (7)$$

$$B_2O_4^{2-} = B_2O_3 + 1/2O_2 + 2e^- \quad (8)$$

$$Na^+ + e^- = Na \quad (9)$$

$$3Na + 2B_2O_3 = B + 3NaBO_2 \quad (10)$$

Based on cyclic voltammetry study [22], $Na_2B_4O_7$-Na_2CO_3 was electrolyzed at -0.8V for 3 h using tungsten wire-graphite-platinum wire three-electrode system at 1223K. The SEM image and EDS analysis of the product collected from the cathode was shown in Figure 9. It was found that boron was produced in the cathode using $Na_2B_4O_7$-Na_2CO_3 as electrolyte. The impurities (Figure 9 (a)) coexisted with boron such as O came from molten salts, and Fe was brought in when collecting powder samples.

The boron atom generated by the above reactions was adsorbed on the surface of nickel substrate and reacted with nickel to form nickel borides. The reaction equations and their ΔG^0-T relationship were calculated by HSC Chemistry6.0 and shown in Figure 10. It can be seen that the boronizing reactions are thermodynamically spontaneous at the experimental temperature (1193-1243K).

3.6. Borided layer growth kinetics

Depending on the boronizing temperature and time, the thickness of the borided layers ranged from 71 to 184 μm. The morphology and thickness of the

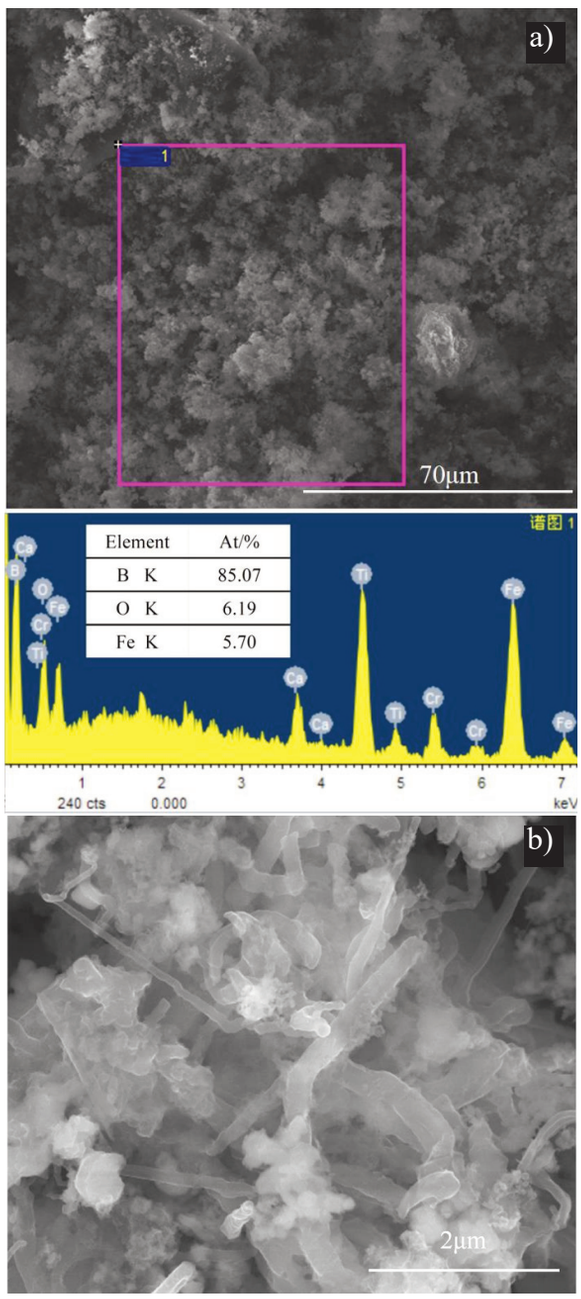

Figure 9. *EDS analysis (a) and SEM image (b) of the cathodic product from $Na_2B_4O_7$-Na_2CO_3 (-0.8V, 3h, 1223K)*

Table 1. *Fitting results of the polarization curve*

Sample	β_a	β_c	R_p	i_{corr}	E_{corr}	Corrosion Rate
	/V	/V	/Ω·cm^2	/A·cm^{-2}	/V	/(mm·a^{-1})
Pure nickel	0.5481	0.4848	4.36×10^2	2.56×10^{-4}	-0.45699	3.0051
Boronized sample	0.3741	0.4662	3.34×10^3	2.66×10^{-5}	-0.31959	0.31326

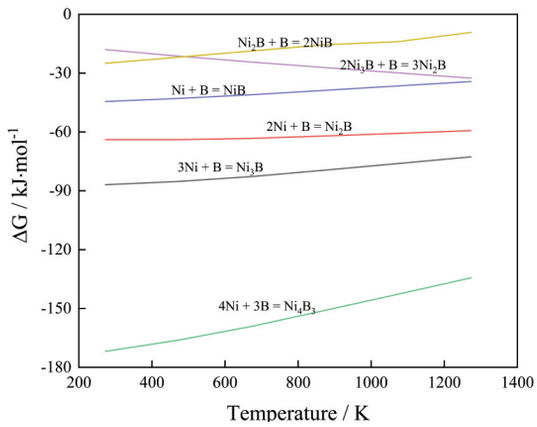

Figure 10. *Gibbs Free Energy for reactions between Ni and B at different temperatures*

borided layer formed under different conditions were observed by SEM, as shown in Figure 11. As the outer silicon rich borides layer accounts for only a small part of the total borided layer, growth kinetics of the borided layer was investigated assuming that the borided layer was composed of nickel borides.

The square variations of the borided layer thickness (d^2) at different temperatures are given as a function of processing time (t) in Figure 12. Apparently, the dependence of the rate of the borided layer formation on time showed a parabolic character at all process temperatures.

From Figure 12 it can be seen that the incubation times exist for 1193, 1223, and 1243K: therefore, the relationship between d and t can be written as Eq (11) based on the parabolic law.

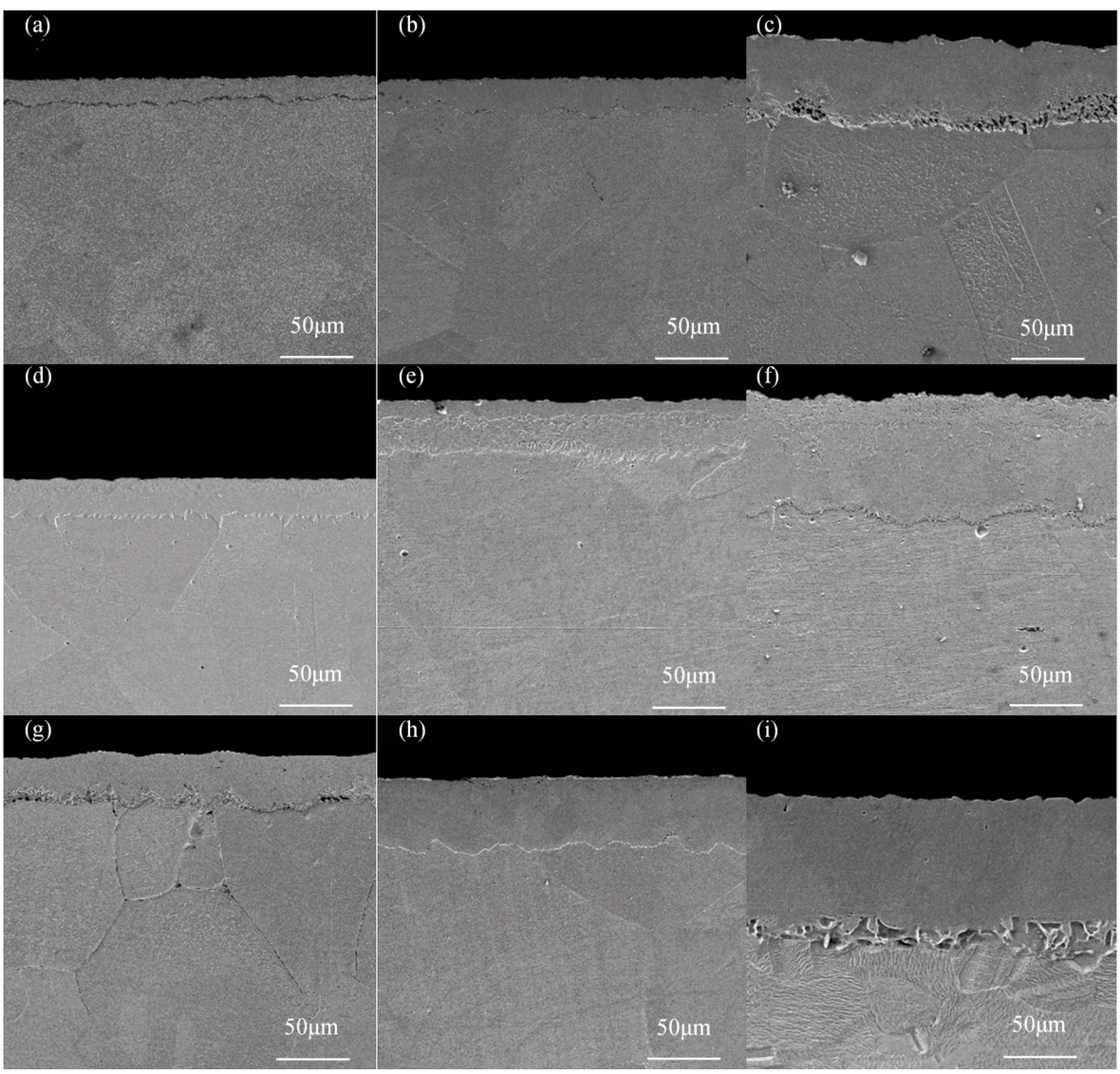

Figure 11. *Cross-sectional SEM images of the boronized sample at different electrolysis temperature and time (a)1193K-1/4h,(b)1193K-1/2h,(c)1193K-1h,(d)1223K-1/4h,(e)1223K-1/2h,(f)1223K-1h,(g)1243K-1/4h,(h)1243K-1/2h,(i)1243K-1h*

$$d^2 = K\ (t - t_0) \quad (11)$$

where d is the thickness of the borided layer, K is the growth rate constant, t is the boriding time, and t_0 is the incubation time in boriding process.

The growth rate constants (K) of the borided layer at different temperatures can be calculated according to Eq (11), hence from the slopes of the straight lines in Figure 12. The data of regression effect test for the relationship between square borided layer thickness (d^2) and time (t) were listed in Table 2. As expected, the diffusion rate of boron atoms into nickel, corresponding to the diffusivity, increased with the process temperatures.

The boride incubation times (t_0) are deduced from the Figure 12 by fitting the experimental boride layer with Eq (11), as shown in Table 3. Here the incubation time means the time needed to form nickel borides. The formation of nickel borides involve at least two steps: the generation of boron atom and the diffusion of boron atom into the nickel crystal to form nickel borides. As stated in part 3.5 that the boron atom can be generated after a series of electrochemical and chemical reactions, time will be needed in this step. In addition, it needs time to finish the diffusion of the newly generated boron into the nickel crystal lattice and to finish the reaction between boron and nickel. It can be seen in Table 3 that the incubation time becomes shorter at a higher temperature. This is because higher temperature is favorable to electrochemical and chemical reactions and to the diffusion of atoms.

The growth rate constant (K) determines the speed of the borided layer formation and depends on the temperature according to Arrhenius equation (Eq (12)), the chemical composition of substrate, and the concentration gradient of boron.

$$K = K_0 exp\left(-Q/(RT)\right) \quad (12)$$

where K_0 is the pre-exponential factor, Q is the activation energy of the borided layer formation, T is the temperature, and R is the gas constant.

The plot of ln$K$ versus reciprocal treatment temperature is linear as shown in Figure 13, and ln$K$ decreases with treatment temperature ($1/T$). The derived formulas between the growth rate constant values (ln$K$) and temperature ($1/T$) was shown in Eq (13).

$$lnK = -(30597.01/T) - 1.650 \quad (13)$$

Table 3. *Boride incubation times*

Temperature (K)	Boride incubation time t_0 (s)
1193	778.1
1223	485.5
1243	299.7

Table 2. *Regression effect test for the relationship between borided layer thickness and time (750A/m²)*

Temperature (K)	Adj. R-Square	Equation	K (m²/s)
1193	0.8979	$d^2 = 1.14\times10^{-12}\,t - 8.87\times10^{-10}$	1.14×10^{-12}
1223	0.9394	$d^2 = 2.07\times10^{-12}\,t - 10.05\times10^{-10}$	2.07×10^{-12}
1243	0.9809	$d^2 = 3.20\times10^{-12}\,t - 9.05\times10^{-10}$	3.20×10^{-12}

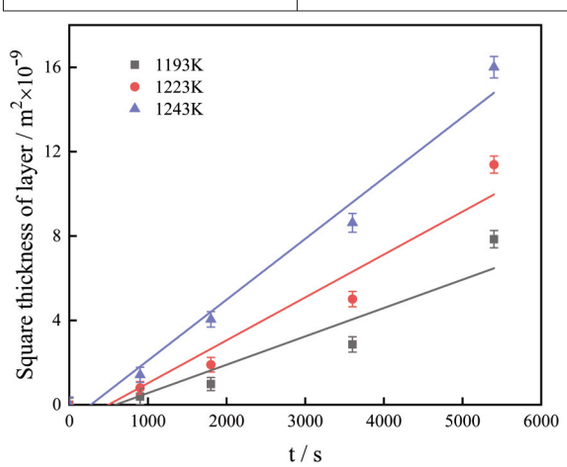

Figure 12. *Curve for relationship between thickness square of the borided layer and electrolysis time*

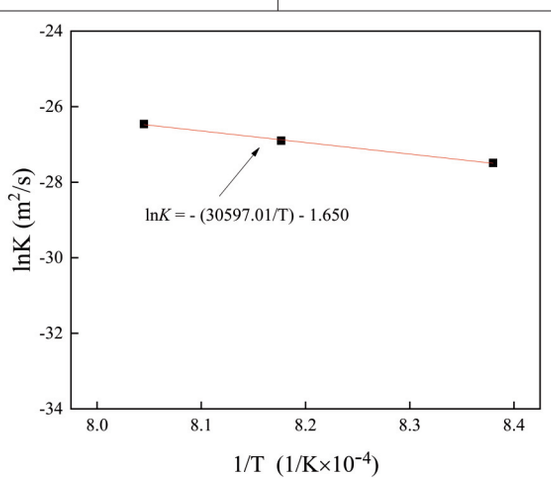

Figure 13. *Relationship Between lnK and 1/T*

Q was determined to be 254.383 kJ/mol, and K_0 to be 0.192 m^2/s.

Hence Eq (11) can be finally rewritten as follows:

$$d = \sqrt{0.192 exp\left(-\frac{254.38\times10^3}{RT}\right)(t-t_0)} \quad (14)$$

The experimental values of thickness obtained at 1223K for 1,2,3 and 4 h (as shown in Figure 6 (a)) can be used to validate Eq (14), the results were shown in Table 4.

Table 4. *Comparison for boriding layer thickness in experiment and from Eq (14)*

No.	Boriding layer thickness (μm) in experiment	Thickness (μm) calculated from Eq (14)
1	71	90
2	150	133
3	175	164
4	184	191

It is seen that the calculated values of thickness are comparable to those obtained experimentally.

As can be seen, the growth rate constant and activation energy of boron diffusion in the boride layer at 1223 K is 2.07×10^{-12} m^2/s and 254.383 kJ/mol, respectively, while Liu [27] reported the different data of 1.6873×10^{-11} m^2/s and 205.3 kJ/mol, respectively. The probable reason for these differences seen in *K and Q* values could be the concentration gradient of boron atoms on the surface (the saturation of substrate surface with boron atoms), as the boronizing method used by Liu [27] is different from what we used.

In addition, the activation energy of 254.383 kJ/mol for the borided layer of nickel is higher than that of titanium (152.02 kJ/mol) [28], indicating that the energy required for the diffusion of boron atoms from one gap position to another in the nickel is higher than in titanium. However, since the order of magnitude of the diffusion coefficient of boron atoms in the nickel is 10^{-12}~10^{-13}, which is higher than that in the titanium (10^{-14}~10^{-15}), the thickness of the borided layer on nickel surface is larger than that on titanium under similar boronizing conditions.

4. Conclusions

The molten salt electrolysis was applied for the boronizing of pure nickel. When using silicon carbide crucible in electrolysis, the borided layer formed on the surface of nickel are mainly composed of Ni_2B and Ni_3B, with the upper zone rich in silicon.

When the electrolysis temperature is 1223 K, the electrolysis time is 1h and the current density is 750 A / m^2, the thickness of the borided layer is about 71 μm, the hardness of the silicon rich nickel borides in the upper zone is 966 HK, which is a little lower than that of the nickel borides (992-1008 HK) in the inner zone. After 4 h of electrolysis, the thickness of the borided layer is about 184 μm, with a surface hardness of 1755 HK, which is about 8.7 times that of the pure nickel. (199 HK).

Electrochemical impedance spectroscopy analysis showed that the corrosion resistance of boronized sample is better than that of pure nickel. Polarization curve analysis showed that the self-corrosion current density of boronized sample (2.66×10^{-5} A/cm^2) was lower than that of nickel matrix (2.56×10^{-4} A/cm^2), and the self-corrosion potential (-0.32 V) was higher than that of nickel matrix (-0.46 V).

The diffusion coefficients of boron in nickel boride at different temperatures can be calculated by the growth kinetics of the boride layer, i.e. $K_{1193} = 1.14\times10^{-12}$ m^2 / s, $K_{1223} = 2.07\times1^{-12}$ m^2/s, $K_{1243} = 3.20\times10^{-12}$ m^2/s. The activation energy for boron diffusion in the boride layer was determined to be 254.383 kJ/mol. An equation ($d = \sqrt{0.192 exp\left(-\frac{254.38\times10^3}{RT}\right)(t-t_0)}$) was obtained to estimate the thickness of the boride layer at 1223 K, and the empirical relation was validated by comparing the experimental thicknesses of boride layer with the values calculated from the equation.

Acknowledgments

This work was supported by the National Natural Science Foundation of China (No.51404186).

Credit author statement

Bixia Wang: Conception and design of study, interpretation of data, drafting the manuscript ; Wenlong Yuan: Acquisition and analysis of data, response to the reviewr, manuscript revision; Ziyu Wang: Validation, Conceptualization, Methodology; Jianxin Li: Data curation, interpretation of data; Hongzhou Ma: Revising the manuscript critically for important intellectual content; Yonghui Song: Revising the manuscript critically for important intellectual content

Declaration of interests

The authors declare that they have no known competing financial interests or personal relationships that could have appeared to influence the work reported in this paper.

References

[1] I. Gunes, M. Keddam, R. Chegroune, M. Ozcatal, Growth kinetics of boride layers formed on 99.0% purity nickel, Bulletin of Materials Science, 38 (4)

(2015) 1113-1118.
https://doi.org/10.1007/s12034-015-0931-y

[2] Y. Huang, J. Chen, M. Zhang, X. Zhong, H. Wang, Q. Li, Electrolytic Boronizing of Titanium in $Na_2B_4O_7$-20%K_2CO_3, Materials and Manufacturing Processes, 28 (12) (2013) 1310-1313.
https://doi.org/10.1080/10426914.2013.840912

[3] H. Liu, W. Liu, H. Qu, S. Liu, Valence Electron Structures of TiB and TiB_2 and hardening on boronizing layer of TC4 alloy, Rare Metal Materials and Engineering, 44 (5) (2015) 1139-1143). (In Chinese)

[4] D. Mu, Z. Hu, B. Shen, Microstructure and properties of borosiliconized pure nickel, Rare Metal Materials and Engineering, 44 (8) (2015) 1979-1984.) (In Chinese)

[5] M. Kulka, N. Makuch, M. Popławski, Two-stage gas boriding of Nisil in N_2-H_2-BCl_3 atmosphere, Surface and Coatings Technology, 244 (2014) 78-86.
https://doi.org/10.1016/j.surfcoat.2014.01.057

[6] M. Kulka, N. Makuch, A. Pertek, L. Małdziñski, Simulation of the growth kinetics of boride layers formed on Fe during gas boriding in H_2-BCl_3 atmosphere, Journal of Solid State Chemistry, 199 (2013) 196-203.
https://doi.org/10.1016/j.jssc.2012.12.029

[7] N. Makuch, M. Kulka, A. Piasecki, The effects of chemical composition of Nimonic 80A-alloy on the microstructure and properties of gas-borided layer, Surface and Coatings Technology, 276 (2015) 440-455.
https://doi.org/10.1016/j.surfcoat.2015.06.031

[8] N. Makuch, Influence of nickel silicides presence on hardness, elastic modulus and fracture toughness of gas-borided layer produced on Nisil-alloy, Transactions of Nonferrous Metals Society of China, 31 (3) (2021) 764-778. https://doi.org/10.1016/S1003-6326(21)65537-1

[9] R. Kouba, M. Keddam and M. Kulka, Modelling of paste boriding process, Surface Engineering, 31 (8) (2015) 563-569.
https://doi.org/10.1179/1743294414Y.0000000357

[10] N. Makuch, M. Kulka, P. Dziarski, S. Taktak, The influence of chemical composition of Ni-based alloys onmicrostructure and mechanical properties of plasma paste boridedlayers, Surface and Coatings Technology, 367 (2019) 187-202.
https://doi.org/10.1016/j.surfcoat.2019.03.042

[11] I. Gunes, I. Taktak, C. Bindal, Y. Yalcin, S. Ulker, Y. Kayali. Investigation of diffusion kinetics of plasma paste borided AISI 8620 steel using a mixture of B_2O_3 paste and B_4C/SiC, Sadhana, 38 (2013) 513-526.
https://doi.org/10.1007/s12046-013-0136-2

[12] M. Keddam, R. Chegroune, M. Kulka, N. Makuch, D. Panfil, P. Siwak, S. Taktak Characterization, tribological and mechanical properties of plasma paste borided AISI 316 steel, Transactions of the Indian Institute of Metals, 71(1) (2018) 79-90.
https://doi.org/10.1007/s12666-017-1142-6.

[13] A. Günen, Properties and high temperature dry sliding wear behavior of boronized inconel 718, Metallurgical and Materials Transactions A-Physical Metallurgy and Materials Science, 51 (2) (2020) 927-939.
https://doi.org/10.1007/s11661-019-05577-3

[14] A. Haddad, N. Chiker, M. Abdi, M.E.A. Benamar, M. Hadji, M.W. Barsoum, Microstructure and tribological properties of boronized TizAlC MAX surfaces, Ceramics International, 42 (14) (2016) 16325-16331.
https://doi.org/10.1016/j.ceramint.2016.07.189.

[15] İ. Türkmen, A. Korkmaz, Microstructural and mechanical characterization of powder-pack boronized Incoloy A286 superalloy, Surface Topography: Metrology and Properties, 9 (1) (2021) 015002.
https://doi.org/10.1088/2051-672X/abd9a8

[16] A. Çalik, Effect of Powder Particle Size on the Mechanical Properties of Boronized EN H320 LA Steel Sheets, ISIJ International, 53 (1) (2013) 160-164.
https://doi.org/10.2355/isijinternational.53.160

[17] G. Kartal, O. L. Eryilmaz, G. Krumdick, A. Erdemir, S. Timur, Kinetics of electrochemical boriding of low carbon steel, Applied Surface Science, 257 (15) (2011) 6928-6934.
https://doi.org/10.1016/j.apsusc.2011.03.034

[18] V. Sista, O. Kahvecioglu, O. L. Eryilmaz, A. Erdemir, S. Timur, Electrochemical boriding and characterization of AISI D2 tool steel, Thin Solid Films, 520 (2011) 1582-1588.
https://doi.org/10.1016/j.tsf.2011.07.057

[19] M. Eroglu, Boride coatings on steel using shielded metal arc welding electrode: Microstructure and hardness, Surface and Coatings Technology, 203 (16) (2009) 2229-2235.
https://doi.org/10.1016/j.surfcoat.2009.02.010

[20] L. Segers, A. Fontana, R. Winand, Electrochemical boriding of iron in molten salts, Electrochim Acta, 36 (1) (1991) 41-47.
https://doi.org/10.1016/0013-4686(91)85177-9

[21] V. Sista, O. Kahvecioglu, G. Kartal, Q. Z. Zeng, J. H. Kim, O. L. Eryilmaz, A Erdemir, Evaluation of electrochemical boriding of Inconel 600, Surface and Coatings Technology, 215 (2013) 452-459.
https://doi.org/10.1016/j.surfcoat.2012.08.083

[22] B. Wang, L. Cheng, D. Tian, X. Ma, Boriding of TC4 titanium alloy by molten salt electrolysis, Rare Metal Materials and Engineering, 45 (3) (2016) 709-714. (In Chinese)

[23] B. Wang, X Ma, D Li, J Li, H Liu, Effects of current density on TiB_2/TiB layer by molten salt electrolysis in $Na_2B_4O_7$-CaCl, melt, Rare Metal Materials and Engineering, 47 (7)(2018) 2120-2125.

[24] D. Mu, B. Shen, C. Yang, X. Zhao, Microstructure analysis of boronized pure nickel using boronizing powders with SiC as diluent,Vacuum, 83 (12) (2009) 1481-1484.
https://doi.org/10.1016/j.vacuum.2009.06.048

[25] H. P. Lyakishev (Author), Q. Guo (Translator), Handbook of metal binary phase diagrams, Beijing: Chemical industry press, 2009 (In Chinese)

[26] C. Cao, Pinciple for corrosion electrochemsitry, Beijing:Chemical industry press, 2009 (In Chinese)

[27] H. Liu, Investigation and property analysis of electric field assisted boriding process on pure nickel substrates, Guangzhou: South China University of Technology, 2020 (In Chinese)

[28] B. Wang, J. Li, X. Ma, H. Ma, Z. Li, Growth kinetics of boride layer produced by molten salt electrolytic boriding on TA2, The Chinese Journal of Nonferrous Metals, 29 (1) (2019) 131-136. (In Chinese)

KARAKTERIZACIJA I KINETIKA RASTA BORIDNOG SLOJA FORMIRANOG NA ČISTOM NIKLU ELEKTROLIZOM RASTOPA SOLI

B.-X. Wang*, W.-L. Yuan, Z.-Y. Wang, J.-X. Li, H.-Z. Ma, Y.-H. Song

Šian univerzitet arhitekture i tehnologije, Fakultet za metalurško inženjerstvo, Šian, Kina

Apstrakt

Elektroliza rastopa soli korišćena je za boronizaciju nikla sa $Na_2B4O_7{\cdot}10H_2O$-Na_2CO_3 kao elektrolitom, i prikazana je karakterizacija i kinetika rasta boridnog sloja. Eksperiment je izveden u silicijum karbidnom tiglu na temperaturama od 1193 K, 1223 K i 1243 K u trajanju od 1 h, 2 h, 3 h i 4 h. Morfologija i faze formirane na površini čistog nikla analizirane su uz pomoć skenirajuće elektronske mikroskopije (SEM), energijsko-disperzivne rendgenske spektroskopije (EDS) i rendgenske difrakcione analize (XRD). Tvrdoća površine i otpornost na koroziju boroniziranog uzorka testirani su pomoću uređaja za merenje mikrotvrdoće i elektrohemijske radne stanice, pojedinačno. Boridni sloj se sastojao od nikl borida i njegova debljina kretala se od 71 do 184 μm. Posle boronizacije u trajanju od 1 h, tvrdoća borida bogatih silicijumom bila je 966 HK, što je nešto niže u odnosu na boride nikla (992-1008 HK); tvrdoća površine dostigla je 1755 HK posle 4 h elektrolize. Analize elektrohemijskom impedancijskom spektroskopijom pokazale su da je otpornost na koroziju boroniziranog uzorka bolja nego kod čistog nikla. Kinetika rasta boridnog sloja proučavana je analiziranjem odnosa između debljine boridnog sloja i vremena uz pomoć matematičke metode. Zatim je konstanta koeficijenta difuzije atoma bora u niklu pri temperaturi od 1193 K, 1223 K i 1243 K izračunata i dobijena je jednačina za procenu debljine boridnog sloja.

Ključne reči: *Čist nikl, Boriranje; Elektroliza otoplene soli; Kinetika; Tvrdoća površine*